URTeC Control ID Number: 1581818

Correlation of Azimuthal AVO Gradient Anisotropic Analysis and Curvature on Prediction of Fractures on Barnett Shale

Shiguang Guo*, Bo Zhang, Tengfei Lin, Kurt J. Marfurt

Summary

Barnett Shale is a major hydrocarbon source rock in the Fort Worth basin. As one of the most fully developed shale gas plays in North America, knowing the fracture orientation and density in Barnett shale is critical for fracturing during horizontal drilling. In our study, the main objective is to predicate the azimuth and density of natural fractures of the Barnett Shale.

We migrate our seismic data by a new binning approach that sort the data by azimuth. We calculate AVO gradient from prestack gathers for each azimuth bin. By comparing the azimuthal AVO gradient variation, we generate the AVO gradient anisotropy for prediction of natural fractures.

Strike-slip faults are known to modify the subsurface stress regime. We map faults using both the strike and magnitude of the most-positive and most-negative principal curvatures and visually correlate them to AVAz. There is high correlation between positive curvature and high anisotropy density. Finally, we generate a vector correlation between AVAz and the two curvatures, and find that perpendicular relationship between the most negative curvature and AVAz vector.

Introduction

The Fort Worth Basin has been the interested object so far, because its role as one of the most important early shale gas plays. Although high TOC property of Barnett Shale makes it a good source rock, it is characterized by low permeability. Hydraulic fracture is required to provide pathways for fluid flow and increase the permeability. It has been a problem for the choice of the fracturing, so accurately mapping the density and azimuth of natural fractures and stress field can be essential for the production and horizontal hydraulic fracture choice.

Significant effort has been done on seismic response for imaging the fractures. Direct measures of fractures include Amplitude vs. Azimuth (AVAZ) (Ruger, 1998; Goodway et al., 2007b) and azimuthal velocity anisotropy (Sicking et al., 2007; Roende et al., 2008; Jenner, 2001). Geometric attributes over post-stack data include coherence and curvature also has been used for fracture prediction (Chopra et al., 2007; Blumentritt et al., 2006; Thompson et al. 2010, Yanxia et al., 2010). AVO gradient has been regarded as a method for gas

detection. The AVO response to fractures will occur at ray path directions not parallel to the fractures. The reflectivity response parallel to fracture strike is close to that of the unfractured rock matrix (Ruger and Tsvankin, 1995; Ruger, 1997). Heloise et al. (1999) found the AVO gradients.measured normal to fractures at known water wet zones were near zero or negative.

In this study, we migrate our seismic data into different azimuths using a new binning approach that is developed by Perez and Marfurt (2008). This new binning allows us to identify the image contribution from out-of-the-plane steeply dipping reflectors, fractures, and faults. Next we inverse the AVO gradient for different azimuth prestack gathers, then we fit sinusoids to the four AVO gradient volumes and obtain the maximum AVO gradient direction. By performing anisotropic analysis on these four AVO gradient volumes, we predict fracture azimuth and density. In addition, we get most negative curvature over stacked volume, the correlation between negative curvature strike and azimuthal AVO gradient anisotropy is established. At last, gas production map is obtained along 60ms below Barnett Shale base on EUR information from wells available. We establish the correlation between AVO gradient anisotropy and gas production map.

Method

Perez and Marfurt (2008) proposed a new azimuthal binning approach to Kirchhoff prestack migration that sorts output by the azimuth of the average travel path from surface midpoint to subsurface image point, rather than the azimuth between source and receiver (Figure 1). This new binning allows us to identify the image contribution from out-of-the-plane steeply dipping reflectors, fractures, and faults.
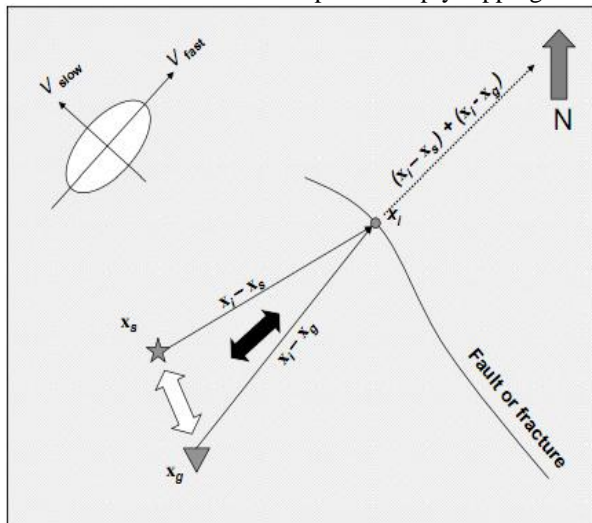

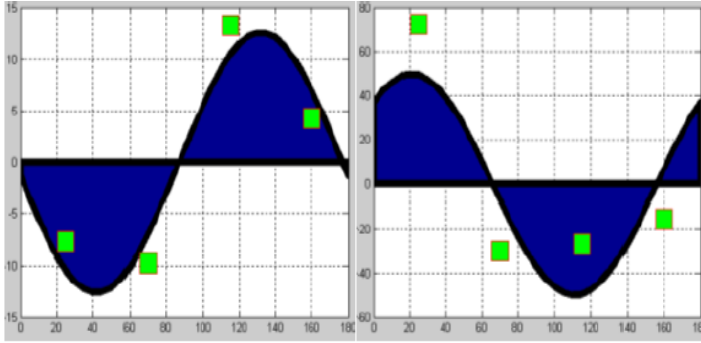Figure 1: New azimuthal binning (after Perez and Marfurt, 2008).

Figure 2: Example of a good sinusoidal fit (a) and bad one (b) by using four samples (after Zhang et al. 2011).

Rueger's (1996) equation for AVAz can be written as

$$R(\theta,\varphi)=A+\{B_{iso}+B_{aniso}\cos[2(\varphi- 2_{sym})]\}\sin^2\theta \quad (1)$$

where $R(\theta,\varphi)$ is the reflectivity at angle of incidence θ and azimuth φ. In the absence of anisotropy, $B_{aniso}=0$, and equation (1) reverts to the well-known AVO equations in terms of slope, B_{iso}, and intercept, A. Note the azimuthal anisotropy plays an increasingly stronger role larger angles of incidence, as indicated by the $\sin^2\theta$ coefficient. It is critical to account for VVAz effect prior to application of AVAz. We therefore "register" the different azimuthally limited volumes by picking the Viola and flattening.

 We improve slightly upon the robustness of normal AVAz analysis by computing the principal component of $R(\theta,\varphi)$ within a 20 ms window, which is equivalent of Karhunen-Loeve filtering the azimuthal gathers. Otherwise, we follow Zhang et al. (2011), and fit equation (1) to the azimuthally limited AVO computations, resulting in the magnitude of the minimum and maximum AVO gradient and their strike, as well as an estimate of the goodness of the fit (Figure 2).

Example

Fort Worth Basin (FWB) is a shallow foreland basin, located in north Texas. The mostly dolomitic Ellenburger Group exhibits high porosity resulting from the development of karst features, and is often a water-bearing formation that can destroy shallower gas production in the shale reservoir through connectivity of either natural or induced fractures. In the area of study, the Mississippian Barnett Shale was deposited directly over the eroded Viola limestone strata, on a shelf or in a basin area marginal to the Ouachita geosyncline. The Barnett Shale sequence consists of alternating shallow marine limestone black, organic rich shale. In the eastern side of the FWB, the Barnett shale can be subdivided into an upper- and a lower-interval unit interbedded by a dark limestone interval, known as the Forestburg limestone. The Forestburg is absent in the south and west of this survey and is not an exploration target. However, it forms an effective fracture barrier to contain the induced hydraulic fractures in the gas wells. The presence of glauconite and phosphate material indicates slow deposition under reducing conditions (Aktepe, 2007).
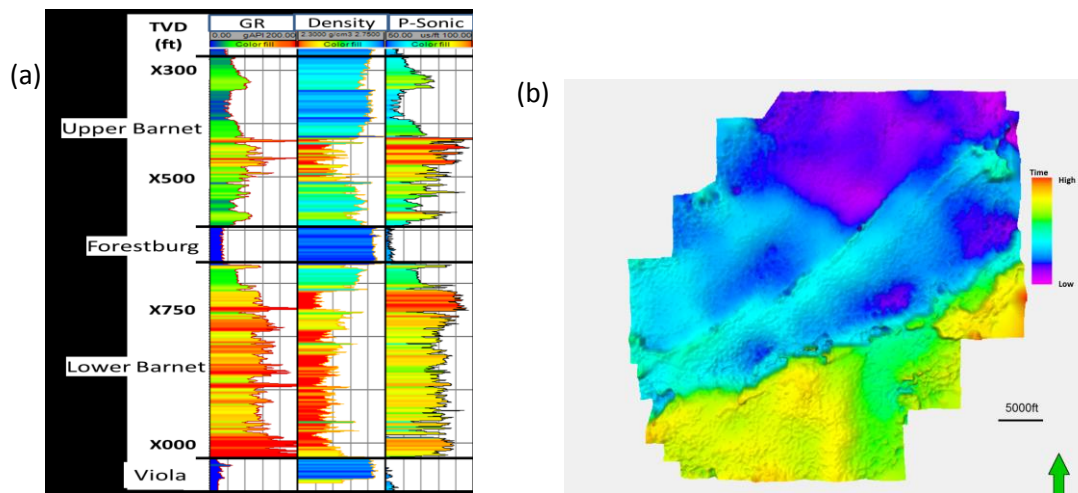

Figure 3, (a) A representative log through the Barnett Shale within the survey. (b) Time structure map of the top of Lower Barnett Shale.

Figure 4 shows four azimuthally limited stacked volumes. Note the stacked volumes at 90° and 135° show higher resolution than those at 0° and 45° around the fault zone. The azimuths 0° and 45° are approximately parallel to the fault plane azimuth, while azimuth 90° and 135° is perpendicular to the strike of the faults, and more reflection energy from the fault plane in these two azimuths. In addition, the signal-to-noise ratio is better in stacked volume from 90° and 135°.
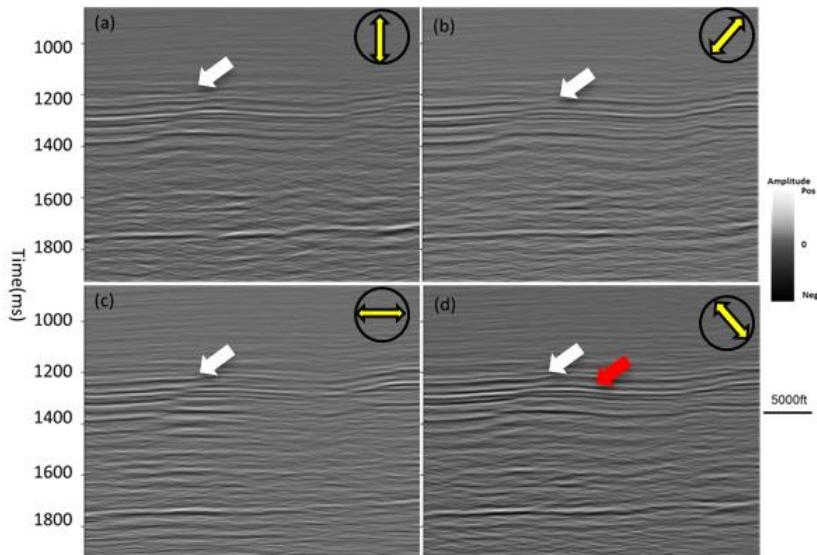
Figure 4: Vertical slice through stacked volumes along profile AA' from (a) azimuth 0 ^{o}, (b) 45°, (c)90°, (d)135°. White arrows denote faults, red arrow denotes the lower Barnett shale. Note difference of faults lineaments from different azimuth stacked volume.

Figure 5 shows vertical slice through AVO gradient volumes along profile AA'. Note the difference of AVO gradient from these four azimuths, there is significant AVO gradient anomaly around fault zone in the AVO gradient volume of azimuth 90° and 135° compared to the azimuth of 0° and 45°. Figure 6 shows Horizontal slices 60 ms below the top of lower Barnett through AVO gradient volume, the negative gradient is more dominated on the upper part from 0° and 45° compared with 90° and 135°. This pattern may be correlated with the southwest to northeast direction for dominated natural fractures. Figure 6 show horizontal slices 20 ms below the top of lower Barnett Shale through AVO gradient volume from different azimuth. The negative gradient is stronger in the upper part from 0° and 45° compared with 90° and 135°. Figure 7 shows the anisotropy map calculated from AVO gradient, as well as the most negative curvature, we high correlation between positive curvature and high anisotropy density.
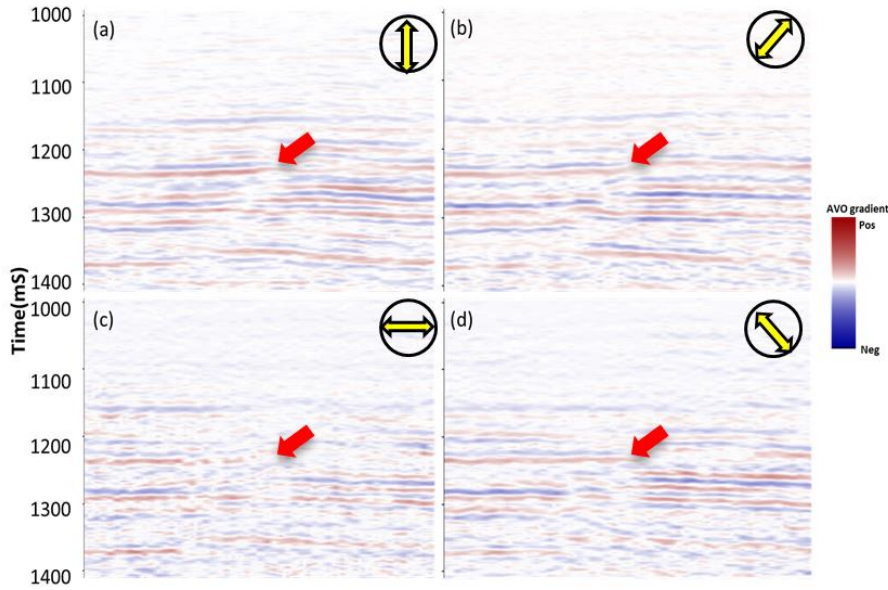
Figure 5: Vertical slice through AVO gradient volumes along profile AA' from azimuth (a) 0 °, (b) 45°, (c) 90°, (d) 135°. The red arrows denote AVO gradient anomaly around faults zone. Note difference of AVO anomaly around faults lineaments from different azimuth stacked volume.
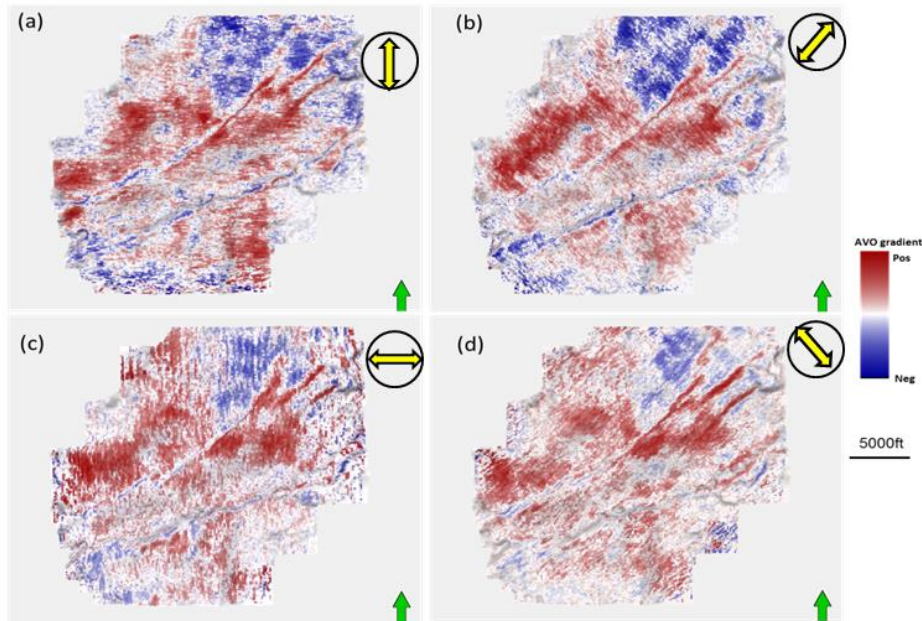

Figure 6: Horizontal slices 20 ms below the top of lower Barnett Shale through AVO gradient volume from azimuth (a) 0°, (b) 45°, (c) 90°, (d) 135°. Note difference of faults lineaments from different azimuth stacked volume.
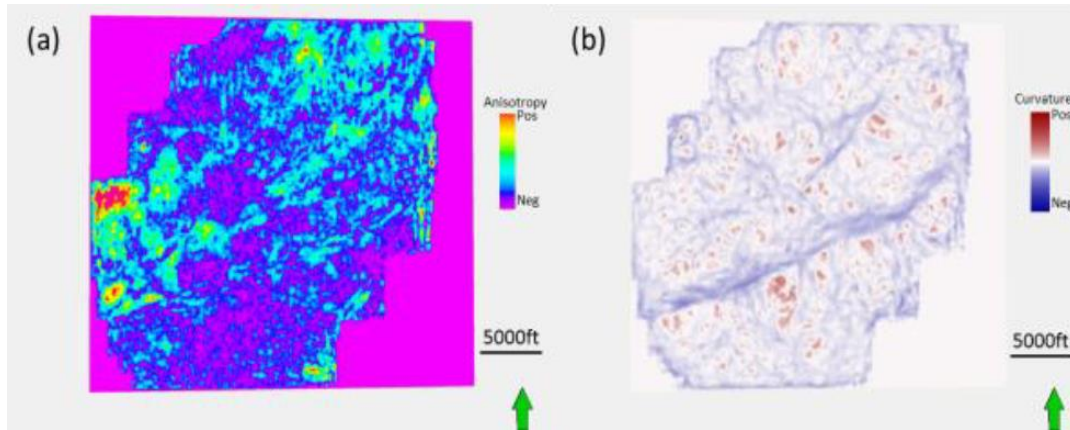
Figure 7, Phantom horizon slices 20 ms below the top of the Lower Barnett Shale through (a) anisotropy, (b) most negative curvature.

Numerical Correlation of Vector Attributes

Both AVAz and the strike and magnitude of the most negative structural curvature are vectors. Since Guo et al. (2010) observed a perpendicular relationship between curvature and VVAz vectors, we do not wish to take a simple inner product between vectors **a** and **b**, but rather

$|\mathbf{c}|=|\mathbf{a}||\mathbf{b}|$, and   (2)

$\arg(\mathbf{c})=\arg(\mathbf{a})-\arg(\mathbf{b})$.   (3)

where $<90^0<\arg(\mathbf{c})\leq90^0$.

Where vector **a** denotes curvature and **b** denotes anisotropy. Then we can create a new vector **c** based on the equations above.
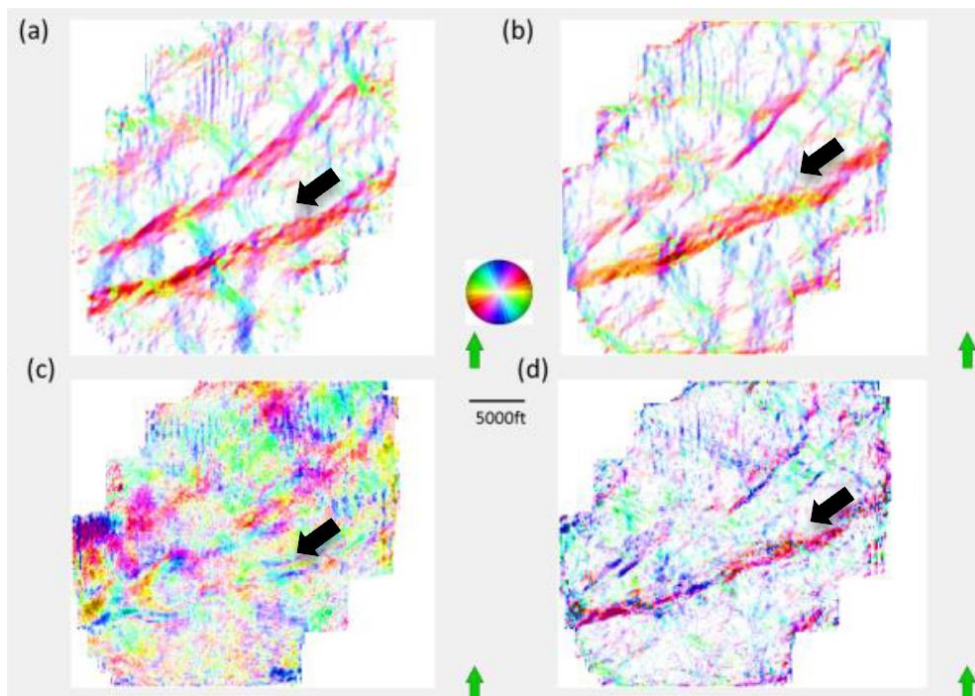

Figure 8, Phantom horizon slices 20 ms below the top of the Lower Barnett Shale through (a) strike of most positive curvature modulated by its value, (b) strike of the most negative curvature modulated by its value, (c) strike of AVAz anisotropy modulated by its value, (d) strike of correlation of new vector attributes modulated by its value. Black arrows denote faults zone, note the different attributes response for faults.

We plot these images using a 2D color bar in figure8. Figure 8a and 8b display strike of most positive and negative curvature modulated by its value. Note the difference of faults expression in these two pictures, the fault is most characterized by purple and red color, which points northeast direction in figure 8b, and from figure 8c, we found that faults is most characterized by green color, which is northwest direction. Note that the faults is characterized by purple color in figure 8d, which is new vector attribute, so perpendicular relationship between the most negative curvature and AVAz vector is found.

Conclusions

The azimuthal AVO gradient can be used as a powerful tool to map azimuth and density of fractures in Barnett Shale, there is high correlation between AVO gradient anisotropy high and most positive nature. In addition, we demonstrate that high gas production from mainly Barnett Shale is correlated to high fracture density related to anisotropy high. We can conclude that natural fracture is characterized by anisotropy high, which can provide us reliable insight for the fracturing choice along horizontal well.

In near future, we will use the same method on one survey after hydraulic fracture performed in the same survey, and to test azimuthal AVO gradient anisotropy response on induced fractures.

Acknowledgements

References

Aki, K., and P. G. Richards, 1980, Quantitative seismology: Theory and methods: W. H. Freeman and Co.

Akepe, S., 2007, Depth imaging of basement control of shallow deformation; Application to Fort Worth Basin and Teapot Dome data sets: M.Sc. Thesis, University of Houston.

Blumentritt, C. H., 2008, Highlight volumes: Reducing the burden in interpreting spectral decomposition data: The Leading Edge, **27**, 330-333.

Chopra, S., and K. J. Marfurt, 2007, Seismic attributes for prospect identification and reservoir characterization: Society of Exploration Geophysicists, Tulsa, OK, 456p.

Guo, Y., 2010, Seismic attribute illumination of the Woodford Shale, Arkoma Basin. Oklahoma: M.Sc. Thesis, The University of Oklahoma.

Guo, H., K. J. Marfurt, S. E. Nissen, and E. C. Sullivan,2010, Visualization and characterization of structural deformation fabric and velocity anisotropy: The leading Edge, 29, 654-660

Goodway W., J. Varsek, and C. Abaco, 2006, Practical applications of P-waveAVO for unconventional gas Resource Plays-1 Seismic petrophysics and isotropic AVO: CSEG Recorder Special Edition 2006.

Lynn, H. et al. 1999, P-wave and S-wave azimuthal anisotropy at a naturally fractured gas reservoir, Bluebell-Altamont Field, Utah: Geophysics, **64**, 1312-1328.

Hunt, L., S. Reynolds, T. Brown, S. Hadley, H. James, J.Downton, and S. Chopra, 2010, Quantitative estimate offracture density variations in the Nordegg with azimuthalAVO and curvature: a case study: The Leading Edge, **29**,1122-1137.

Jenner, E., 2001, Azimuthal anisotropy of 3-D compressional wave seismic data, Weyburn field, Saskatchewan, Canada: Ph.D. dissertation, Colorado School of Mines.

Perez, G. and K. J. Marfurt, 2008, New azimuthal binning for improved delineation of faults and fractures: Geophysics, **73**, S7-S15.

Richards, P. G., and C. W. Frasier, 1976, Scattering of elastic wave from depth-dependent inhomogeneities: Geophysics, **41**, 441–458.

Roende, H., C. Meeder, J. Allen, S. Peterson, and D. Eubanks, 2008, Estimating subsurface stress direction and intensity from subsurface full azimuth land data: 78th Annual International Meeting, SEG, Expanded Abstracts, 217-220

Rueger, A., and I. Tsvankin, 1995, Azimuthal variation of AVO response for fractured reservoirs: 65th Ann. International Meeting, SEG, Expanded Abstracts, 1103-1106.

Rueger, A., 1997, P-wave reflection coefficients for transversely isotropic models with vertical and horizontal axis of symmetry: Geophysics, **62**, 713-722.

Rueger, A., 1998, Variation of P-wave reflectivity with offset and azimuth in anisotropic media: Geophysics, **63**, 935-947.

Sicking, C., S. Nelan and W. Mclain, 2007, 3D azimuthal imaging: 77th Annual International Meeting, SEG, Expanded Abstracts, 2364-2367.

Thompson, A., J. Rich, and M. Ammerman, 2010, Fracture characterization through the use of azimuthally sectored attribute volumes: 80th Annual International Meeting, SEG, Expanded Abstracts, 1433-1436.

Zhang, K., B. Zhang, J. T. Kwiatkowski, and K. Marfurt, 2010, Seismic azimuthal impedance anisotropy in the Barnett Shale: 80th Annual International Meeting of the SEG, Expanded Abstracts, 273-277.